DEVELOPMENT OF ELECTROSPUN NANOFIBRES CONTAINING IBUPROFEN-GRAFTED NANOCRYSTALLINE CELLULOSE FOR DERMAL DELIVERY

ABDULSALAM QAHTAN AHMED AL-MASHHADANI

UNIVERSITI SAINS MALAYSIA

2022

DEVELOPMENT OF ELECTROSPUN NANOFIBRES CONTAINING IBUPROFEN-GRAFTED NANOCRYSTALLINE CELLULOSE FOR DERMAL DELIVERY

by

ABDULSALAM QAHTAN AHMED AL-MASHHADANI

Thesis submitted in fulfilment of the requirements
for the degree of
Doctor of Philosophy

September 2022

ACKNOWLEDGEMENT

First and foremost, praises and thanks to the God almighty for granting me the strength and capability to complete this work.

With great pleasure, I would like to acknowledge with my deepest appreciation my supervisor, Dr. Goh Choon Fu, for his valuable assistance and being a super-great mentor who advised me and guided me in my Ph.D journey.

I would like to express my warm thanks to my wonderful co-supervisors including Associate Professor Dr. Chan Siok Yee, Associate Professor Dr. Cheu Peng Leh and Dr. Lee Chong Yew, for their support, help and endless motivation throughout my research project.

My love and appreciation to my lovely family; my amazing mother, Bushra Fadhil, my wonderful father, Qahtan Ahmed and my gorgeous sisters, Mais and Areej, for their encouragement and continuous support throughout my life.

Also, I am indebted to my friends, Bilal Alrimawi, Fadi Ghassan, Mohammad Althiabat, Ghazi Aljabal, Mohammad Dayoob, Omar Khalid, Ahmed Yaseen, Nadeem Alameen, Sadad Alsaqqar and Ahmad Alasas for being my second family during my Ph.D journey.

I would like to express my thanks to all members of the Goh Skin Research Group and Thought Formulation Group. My sincere thanks also go to Wong Li Ching for being a good lab mate. My thanks are also extended to Universiti Sains Malaysia for the financial support via Research University Individual (RUI) Grant Scheme with

Project No: 1001/PFARMASI/8012320 and Project Code: UO1822 (Reference No: 2019/0589).

Finally, my sense of gratitude to one and all who directly or indirectly have lent their hand in this venture.

TABLE OF CONTENTS

LIST OF TABLES

Page

LIST OF FIGURES

Page

LIST OF SYMBOLS

%	Percentage
×	Magnification
°C	Degree Celsius
$\mu S.cm^{-1}$	Microsiemens per centimetre
3D	Three dimensions
A	Acid concentration
B	Reaction temperature
C	Reaction time
cP	Centipoise
J	Flux
k	The number of factors of the design
kg	Kilogram
L	Litter
M	Molarity
m^2	Meter square
mL	Millilitre
mm	Millimetre
mV	Millivolt
N	Newton
nm	nanometre
R^2	The coefficient of determination
RH	Relative humidity
rpm	Round per minute
w/v	Weight/volume
w/w	Weight/ weight

LIST OF ABBREVIATIONS

^{1}H NMR	Proton nuclear magnetic resonance
2FI	Two-factor interaction
AGUs	Anhydrous glucopyranose units
ANOVA	Analysis of variance
API	Active pharmaceutical ingredient
ATR-FTIR	Attenuated total reflectance-fourier transform infrared
CCD	Central composite design
CrI	Crystallinity index
CTAB	Cetyl trimethylammonium bromide
CV	Coefficient of variation
DLC	Drug loading capacity
DLE	Drug loading efficiency
DLS	Dynamic light scattering
DoE	Design of experiments
DSC	Differential scanning calorimetry
DTG	Derivative thermogravimetric analysis
DX®12	Design-Expert®12 software
EB	Elongation to break
ES	Electrospun
ES	Electrospun
FTIC	Fluorescein isothiocyanate
HPLC	High performance liquid chromatography
IBU	Ibuprofen
LODP	The level–off degree of polymerisation
MW	Molecular weight

NCC	Nanocrystalline cellulose
NSAID	Nonsteroidal anti-inflammatory drug
OPT	Optimisation
PBS	Phosphate buffer saline
PCL	Polycaprolactone
PDI	Polydispersity index
PHBV	Poly 3-hydroxybutyrate-co-3-hydroxyvalerate
PLA	Poly-ethylene-co-vinyl acetate
PLGA	Poly lactic-co-glycolic acid
PS	Puncture strength
PVA	Polyvinyl alcohol
PVP	Polyvinyl pyrrolidone
RPR	The relative cumulative amount of drug permeated to the cumulative amount of drug release
RSM	Response surface methodology
SD	Standard deviation
SEM	Scanning electron microscopy
TCH	Tetracycline hydrochloride
T_d	Degradation temperature
T_g	Glass transition
TGA	Thermogravimetric analysis
$T_{m\ \text{onset}}$	Melting point
WUC	Water uptake capacity
WVP	Water vapour permeability
XRD	X-ray diffraction

LIST OF APPENDICES

PEMBANGUNAN NANOSERAT ELEKTROPUTAR MENGANDUNGI CANGKUKAN NANOKRISTAL SELULOSA DENGAN IBUPROFEN UNTUK PENGHANTARAN DERMIS

ABSTRAK

Nanobahan menawarkan pelbagai faedah dalam pemberian ubat melalui dermis, termasuk nisbah permukaan-ke-isipadu yang tinggi, dan menambahbaik penyelerasan ubat pada epidermis. Selulosa nanokristal (NCC) adalahpembawa ubat nano yang berpotensi kerana mempunyai kumpulan hidroksil yang banyak pada permukaannya yang menjadikannya sesuai bagi congkukan dengan banyak bahan farmaseutikal aktif. Walau bagaimanapun, penghantaran nanobahan secara dermis memerlukan platform yang sesuai bagi memastikan pengedaran nanobahan yang seragam dalam formulasinya. Objektif tesis ini adalah bagi menyiasat serat nano electroputar yang membawa NCC yang dicantumkan ibuprofen bagi aplikasi sistem penghantaran kulit. Pada mulanya, NCC diasingkan dari pulpa kapok menggunakan teknik hidrolisis asid berganda dengan bantuan reka bentuk komposit pusat bagi mengoptimumkan keadaan tindak balas, iaitu kepekatan asid, suhu dan masa tindak balas. Pada keadaan optimum, NCC yang dihasilkan menunjukkan bentuk seperti batang dengan panjang sebanyak 230.3 ± 39.8 nm, potensi zeta sebanyak -39.7 ± 0.6 mV dan hasil sebanyak 18.8 ± 1.5% dan indeks kristal sebanyak 72.6%. NCC yang dihasilkan kemudian disiasat sebagai suatu pembawa nano cangkukan ibuprofen model ubat untuk penghantaran dermis melalui cantuman kimia. Peningkatan kumpulan karbonil dari 1709 ke 1715 cm^{-1} yang direkodkan dalam spekstroskopi inframerah transformasi Fourier - pantulan jumlah terlaif dan kehilangan isyarat ^{1}H bagi kumpulan karboksil ibuprofen pada 12.85 ppm yang direkodkan dalam

spektroskopi resonans magnet nukleus mengesahkan cantuman NCC dengan ibuprofen. Kandungan ubat NCC yang dicangkukan bersama ibuprofen ialah 185 ± 15µg.mg^{-1}. NCC yang dicantumkan bersama ibuprofen dalam bentuk serbuk mempunyai nilai potensi zeta yang rendah (-18.2 ± 1.4 mV) dengan kecenderungan tinggi bagi pergumpalan di tapak sasaran. Elektroputaran dapat digunakan untuk menghalang pengagregatan nanobahan dengan membekukannya dalam tikar serat polimer dengan taburan yang baik. Di samping itu, formulasi elektroputaran mempunyai tahap fleksibiliti dan lekatan kulit yang tinggi, membolehkan sentuhan kulit yang konsisten. Oleh itu, NCC yang dicangkukan bersama ibuprofen dimasukkan ke dalam tikar nanoserat melalui elektroputaran dengan polimer biodegradasi hidrofilik iaitu polivinil alkohol (PVA). Formulasi elektroputaran dengan NCC yang digabung bersama ibuprofen menunjukkan struktur berliang dengan diameter serat sebanyak 151.9 ± 30.6 nm, kekuatan tusukan sebanyak 0.32 ± 0.16 N.mm^{-2} dan pemanjangan hingga putus sebanyak 22.01 ± 5.15%. Formulasi elektroputaran dengan NCC yang dicantumkan bersama ibuprofen mempamerkan profil pelepasan yang berterusan dengan jumlah kumulatif pelepasan ubat sebanyak 46.5 ± 1.8% selepas 72 jam. Walau bagaimanapun, formulasi polimer tunggal mempamerkan sifat melekat pada kulit yang lemah. Oleh itu, kejayaan profil pelepasan ubat berterusan bagi formulasi hibrid ini dapat ditingkatkan dengan menggunakan polimer campuran. Nisbah yang berbeza bagi campuran PVA/ polivinilpirolidon (PVP) disiasat sebagai matriks polimer elektroputaran bagi NCC yang dicangkukan bersama ibuprofen bagi campuran polimer pada pencirian tikar elektroputaran yang dimuatkan dengan NCC yang dicantumkan bersama ibuprofen. Polimer PVA/PVP mempengaruhi keupayaan pembentukan tikar serat kerana sifat higroskopik PVP. Peningkatan kandungan PVP (> 50%w/w) gagal menghasilkan tikar berserat. Walaupun begitu, kewujudan PVP

dapat meningkatkan kestabilan haba dan biopelekatan kulit bagi formulasi tersebut. Pelepasan ubat dan peresapan kulit bagi semua formulasi elektroputaran yang mengandungi campuran PVA/PVP hampir sama dengan formulasi yang mengandungi polimer PVA tunggal. Nisbah ubat yang meresap melalui kulit kepada ubat yang dilepaskan daripada formulasi pada jam 72 memuncak pada 25%w/v PVP (0.58). Namun, tiada formulasi elektroputaran yang menunjukkan perubahan ketara pada kandungan ubat semasa kajian kestabilan terpecut selama 3 bulan tetapi perubahan morfologi berlaku kerana penyerapan lembapan. Kesimpulannya, tikar serat elektroputaran yang dimuatkan dengan NCC yang dicangkukan bersama ibuprofen menggunakan campuran polimer PVA:PVP pada nisbah 75:25%w/w mempamerkan profil pelepasan ubat yang berterusan dengan sifat fisika kima yang baik dalam penghantaran dermis. Pembawa NCC yang dicangkukan bersama ubat berpotensi untuk digunakan dalam reka bentuk platform pelepasan yang berterusan untuk pelbagai aplikasi farmaseutikal.

DEVELOPMENTOF ELECTROSPUN NANOFIBRES CONTAINING IBUPROFEN-GRAFTED NANOCRYSTALLINE CELLULOSE FOR DERMAL DELIVERY

ABSTRACT

Nanomaterials offer various benefits in dermal drug delivery, including a large surface-to-volume ratio and enhanced drug disposition in the skin. Nanocrystalline cellulose (NCC) is a potential drug nanocarrier due to its abundant surface hydroxyl groups, making it suitable to be grafted with active pharmaceutical ingredients. However, dermal delivery of nanomaterials needs a proper platform to ensure a good distribution in the formulations. The objective of the thesis is to investigate the electrospun nanofibres carrying ibuprofen-grafted NCC for dermal delivery system application. Firstly, NCC was isolated from kapok pulp using multiple acid hydrolysis with the assistance of central composite design to optimise the reaction conditions, namely acid concentration, reaction temperature and time. At the optimum condition, NCC produced showed a rod-like shape with a length of 230.3 ± 39.8 nm, zeta potential of -39.7 ± 0.6 mV, yield of 18.8 ± 1.5% and crystallinity index of 72.6%. After that, the obtained NCC was explored as a nanocarrier for ibuprofen as a model drug for dermal delivery via chemical grafting. The grafting of NCC with ibuprofen was confirmed with upshifting the carbonyl group from 1709 to 1715 cm^{-1} in attenuated total reflection Fourier-transform infrared spectroscopy and disappearance of ^{1}H signal of the carboxyl group of ibuprofen at 12.85 ppm in proton nuclear magnetic resonance spectroscopy. The drug content of ibuprofen-grafted NCC was 185 ± 15 $\mu g.mg^{-1}$. Ibuprofen-grafted NCC in the powder form has a low zeta potential value (-18.2 ± 1.4 mV) with a high tendency to aggregate at the target site.

Electrospinning technique can be used to prevent nanomaterial aggregation by freezing them in a polymeric fibrous mat with a good distribution. Furthermore, electrospun formulation has a high degree of flexibility to skin movements and a high level of skin adhesion, allowing a consistent skin contact. Thus, the ibuprofen-grafted NCC was loaded into nanofibre mats using electrospinning process with a hydrophilic biodegradable polymer – polyvinyl alcohol (PVA). The electrospun formulation with ibuprofen-grafted NCC shows a porous structure with a fibre diameter of 151.9 ± 30.6 nm, puncture strength of 0.32 ± 0.16 N/mm^2 and elongation to break of 22.01 ± 5.15%. The electrospun formulation with ibuprofen-grafted NCC exhibited a sustained release profile with a total cumulative amount of drug release of 46.5 ± 1.8% after 72 h. However, the single polymer formulation exhibits poor skin adhesiveness. Therefore, the success story of the sustained drug release profile from this hybrid formulation can be improved by using a polymer blend. Different ratios of PVA/polyvinylpyrrolidone (PVP) blends were then investigated as an electrospun polymer matrix for ibuprofen-grafted NCC to investigate the effect of polymer blend on the characterisation of ibuprofen-grafted NCC loaded electrospun mat. The PVA/PVP polymer affects the ability of fibre mat formation due to the hygroscopic nature of PVP. Increasing the PVP content (> 50%w/w) failed to produce fibrous mats. Despites, the presence of PVP improved the thermal stability of the formulation and their skin bioadhesiveness. The drug release and permeation of all electrospun formulations with PVA/PVP blends were very similar to those of the single PVA polymer. However, the ratio of skin permeation to drug release at 72 h was peaked (0.58) at 25%w/v of PVP. None of the electrospun formulations exhibited a significant change in the drug content during 3-month accelerated stability study but morphological alterations because of moisture absorption. In summary, the electrospun fibre mats loaded with ibuprofen-grafted

NCC using PVA: PVP polymer blend at the ratio of 75:25%w/w exhibited a sustained drug release profile with favourable physiochemical properties in dermal delivery. The drug-grafted NCC carrier has the potential to be employed for designing a sustained release platform for a variety of pharmaceutical application.

CHAPTER 1

INTRODUCTION

1.1 Overview

Dermal drug delivery system refers to a way of administering a formulation to the skin to treat local disorders. The administration of drugs to the skin bypasses the hepatic first-pass metabolism, avoids plasma level fluctuations and improves patient compliance when compared to the oral route Joshi et al. (2014); (Singhvi et al., 2019). The dermal route is painless and has less systemic toxicity and drug exposure to non-infectious tissue or sites.

Materials derived from natural sources are desirable for biomedical applications, including drug delivery. There is a plethora of research to develop a novel drug carrier that can deliver drugs to their active sites with higher therapeutic effects and less toxicity. New technologies are needed to deliver chemically unstable therapeutic compounds, localise the delivery of potent drugs and improve the compliance of patients.

In general, utilising nanomaterials offer several advantages over other drug delivery systems, such as enhancing the solubility of highly hydrophobic drugs (Uppulurj, 2015), providing sustained drug release (Jayaraman et al., 2015) increasing the stability of therapeutic agents (Laurent et al., 2014) and provide targeted treatments with minimal systemic effect (Steichen et al., 2013). Additionally, the high ratio of surface-area-to-mass of nanocarriers permits greater drug distribution and, subsequently, enhanced site-specific targeting (Patel et al., 2017).

Nanocrystalline cellulose (NCC) is biodegradable, has a large surface area, has abundant surface hydroxyl groups, is biocompatible, non-toxic, renewable and low-cost resource with a high degree of crystallinity and potential for chemical modification (Almashhadani et al., 2022; Amnuaikit et al., 2011). These outstanding properties, especially the abundant surface hydroxyl groups available for the formation of hydrogen bonds make the NCC an attractive drug nanocarrier that provides a sustained drug release effect (Gupta et al., 2020; Jackson et al., 2011; Shaikh et al., 2007; Taheri et al., 2015).

Despite the outstanding properties of NCC, NCC does not receive the attention it deserves as a drug nanocarrier in dermal delivery. There is no published record of the drug-grafted NCC. The drug-grafted NCC as a powder lacks bioadhesive properties on the skin, which reduces stability at the target site. In dermal delivery systems, skin adhesion is crucial due to the skin having very dynamic movement (Kwon et al., 2015). Consequently, electrospun fibre polymeric solid dispersion may be able to solve this problem by allowing drug-grafted NCC to freeze or randomly disperse inside the electrospun fibre with good distribution and preventing nanomaterials from aggregating together (Baghali et al., 2022). Therefore, the focus of the thesis is to investigate the grafting of a model drug, ibuprofen (IBU) to NCC before incorporating it into an electrospun fibre mat as a platform for dermal delivery.

Overall, this chapter provides a fundamental background of the skin structure and a comprehensive understanding of NCC as a promising nanomaterial for dermal drug delivery systems. Also, electrospinning process and the application of skin permeation studies were presented.

1.2 Skin as the route of administration

The skin is the biggest organ in the body, weighing around 3.6 kg in adults, covering a surface area of about 2 m^2 (Arens et al., 2006; Joshi et al., 2014). Therefore, it is an attractive drug delivery pathway.

1.2.1 Skin structure

The skin is essential to protect the human body from the external environment such as pollution, bacterial infections and sunlight (Yuhao Liu et al., 2017). Its structure and thickness vary considerably, but on average, it is around 1.5 mm thick and consists of three layers namely, epidermis, dermis and hypodermis (Figure 1.1) (Yousef et al., 2017).

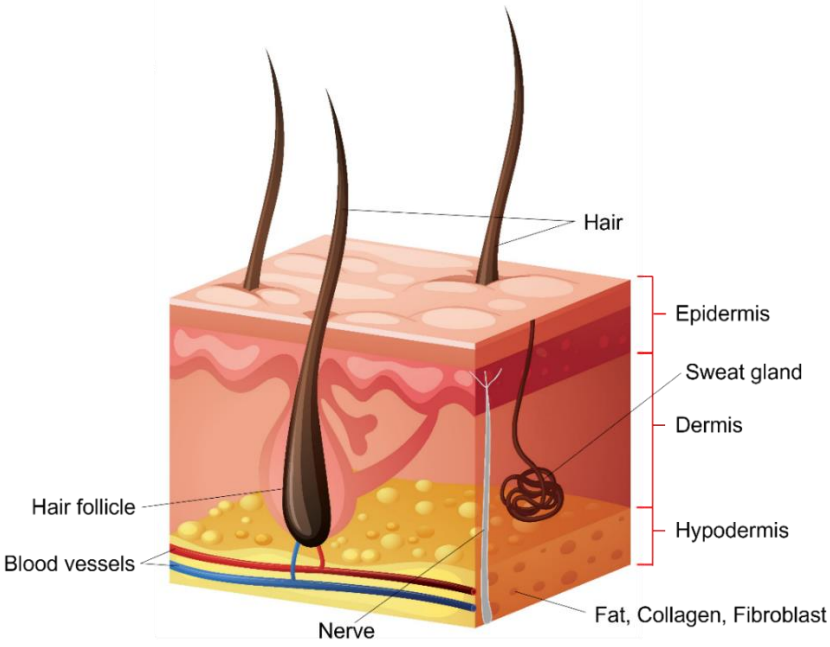

Figure 1.1 Human skin structure. Adapted from MacNeil (2007).

The epidermis is composed of the stratum corneum and the viable epidermis (Yamaguchi et al., 2008). The stratum corneum is the outermost layer of the skin and is made up of a 10-20 µm thick matrix of corneocytes (terminally differentiated

keratinocytes) encased in highly organised lipid layers (Sahle et al., 2015). Also, the stratum corneum has a major influence on the skin barrier function and the poor absorption of medications (Haque et al., 2018). On the other hand, the viable epidermis (usually 0.06 – 0.8 mm thick) is the first layer of living cells below the stratum corneum (Patel et al., 2021). The viable epidermis is made up of around four layers (stratum lucidum, stratum granulosm, stratum spinosum and stratum basale) of keratinocytes (Bouwstra et al., 2003; Hadgraft, 2004).

The dermis is a layer beneath the epidermis that is typically 0.3 – 5 mm thick and is composed of connective tissue, sweat glands, hair follicles and a network of capillaries, lymphatic veins and nerve endings (Bouwstra et al., 2003). While the hypodermis or subcutaneous layer is the deepest layer of the skin. It is a loose, white, fibrous connective tissue that is supported by fat (Walters et al., 2002).

1.2.2 Drug penetration to the skin

Topical (dermal) drug administration is primarily intended to (i) have a local effect, where it may eliminate the need for systemic drug therapy, (ii) lower the total dose required to reach the targeted skin region and (iii) lessen systemic adverse effects (Arens et al., 2006; Joshi et al., 2014). As a result, a variety of active pharmaceutical substances have been delivered dermally, including sunscreens, keratolytic agents, non-steroidal anti-inflammatory drugs, corticosteroids, antibiotics, antivirals, antifungals, antiseptics, local anesthetics and anticancer agents (Goossens et al., 2020; Narasimha Murthy et al., 2010). On the other hand, transdermal drug administration is designed to have a systemic effect, with the skin serving as the drug's entry route into the body (Tanwar et al., 2016).

The penetration of the drug through the stratum corneum is governed by Fick's second law (Trovatti et al., 2012).

$$J = \frac{DCP}{L} \qquad \text{Equation 1.1}$$

where *J* is the flux, *D* is the drug diffusion coefficient, *C* is the concentration of the drug in the formulation, *P* is the partition coefficient of the drug and *L* is the thickness of the stratum corneum.

In general, the use of nanomaterials or nanocarriers as drug delivery systems for topical and transdermal applications exhibits several advantages such as: (i) increasing drug loading in the carrier and drug flux through the skin; (ii) enhancing the solubility of hydrophobic drugs; (iii) offering sustained release pattern of loaded drugs; (iv) improving drug stability via chemical or physical means; (v) providing site-specific treatment (Arens et al., 2006; Joshi et al., 2014; Amoabediny et al., 2018).

The most often utilised nanomaterials for topical drug delivery are polymeric nanoparticles, lipid-based nanoparticles, metal nanoparticles and nanoemulsions (Amoabediny et al., 2018). The following section discusses NCC as a potential nanocarrier for dermal drug delivery.

1.3 Nanocrystalline cellulose

NCC is biodegradable, biocompatible, renewable, non-toxic, has a large surface area, a high amount of surface hydroxyl groups and exhibits potential for chemical modification (Almashhadani et al., 2022; Amnuaikit et al., 2011). As a result, some studies have reported on the use of NCC as a drug nanocarrier for a variety

of active pharmaceutical ingredients (API), including doxorubicin (Jackson et al., 2011), hydroquinone (Taheri et al., 2015) and tetracycline (Wijaya et al., 2017).

NCC can be isolated from the most abundant material on the earth, cellulose (Li et al., 2021). Cellulose is a linear chain consisting of repeated β–D–glucopyranose units connected by β–1,4 glycosidic linkages (Figure 1.2). The assembly of cellulose chains is typically arranged into larger structures known as cellulose microfibrils. These microfibrils are semicrystalline chains containing different domains with varying cellulose chain order: (i) high ordered domain called crystalline regions, (ii) less ordered domain called amorphous regions. Moreover, hydroxyl groups on the surface of β–D–glucopyranose units create a hydrogen-bonded network in the same microfibril and between the different microfibrils, resulting in a larger structural assembly called a bundle of cellulose fibres (Martínez-Sanz et al., 2017).

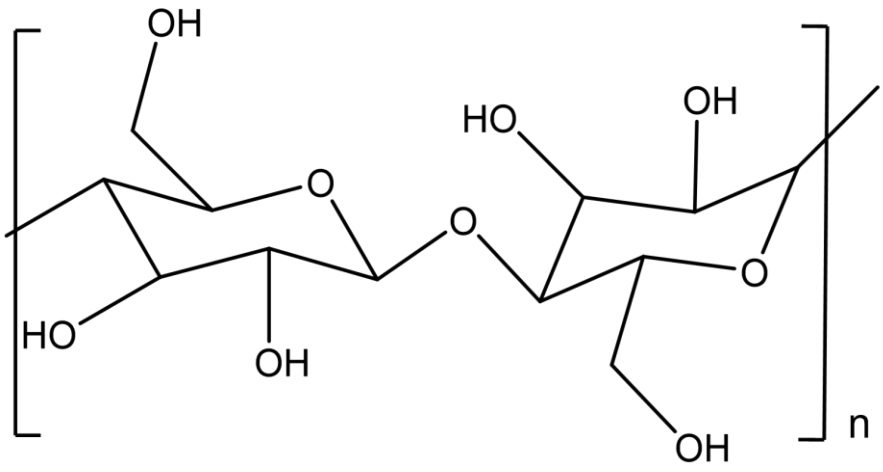

Figure 1.2 Chemical structure of cellulose. Adapted from Marques-Marinho et al. (2013).

1.3.1 Lignocellulosic biomass as cellulose source

Lignocellulosic biomass is the most abundant renewable biopolymer on the earth and mainly includes agricultural residues, forest residues, crops, food wastes and industrial wastes such as wastepaper and demolition waste wood (Ilyas et al., 2019b; Jiang et al., 2019; Zergane et al., 2020b). This promising inexpensive plant–based material is usually discarded, composted, or treated by incineration and landfilling, leading to severe environmental issues such as greenhouse gas emissions, air and water pollution (Broun et al., 2016; Yili Liu et al., 2017).

Lignocellulosic biomass includes several primary components, such as cellulose, hemicellulose and lignin within the complex matrix. The major constituent, cellulose, is mainly localised in the plant cell wall at around 30 – 60% (Borsoi et al., 2020; Tye et al., 2012).

In general, NCC extraction from lignocellulosic biomass can be accomplished in two steps: (i) pretreatment (purification) to remove non-cellulosic components such as lignin and hemicellulose; (ii) removal of cellulose amorphous regions to isolate the crystalline domains as shown in Figure 1.3 (Khalil et al., 2014; Mishra et al., 2019; Phanthong et al., 2018).

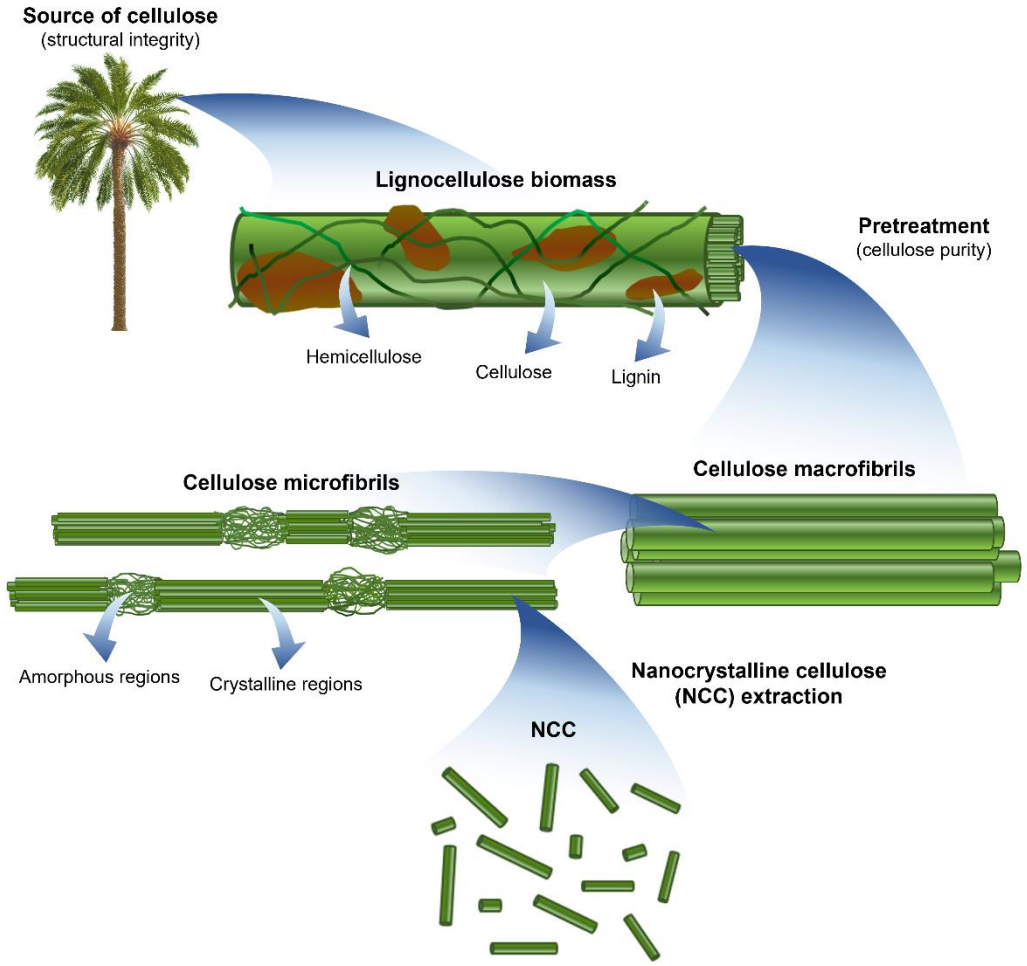

Figure 1.3 General structure of lignocellulose biomass and NCC. Adapted from Almashhadani et al. (2022).

1.3.1(a) Kapok fibres

Kapok fibres are obtained from the seed fibres of kapok tree (*Ceiba pentandra*). The kapok tree is fast growing; within four to five years, kapok becomes productive, and its economic lifespan is approximately sixty years. Under ideal circumstances, a tree can produce 330–400 fruits each year, along with 15–18 kg of fiber and 30 kg of seeds (Tye et al., 2016). In Malaysia, kapok fibres are traditionally used as a filler for mattresses, beds, pillows and dolls. It has historically been planted in village regions (Ansell et al., 2009; Majid et al., 2018). Additionally, kapok fibres

are a common cellulosic fibre with a thin cell wall and a big lumen and the hollow nature of kapok fibres distinguishes them from other natural fibres (Zheng et al., 2015).

To our knowledge, only one work has been published by Mohamed et al. (2017) on the isolation of NCC from kapok fibres (Table 1.1). As a result, it is worthwhile to continue exploring this locally available biomass with a high cellulose content (53 – 64 %) (Draman et al., 2014; Liu et al., 2012). Additionally, the creation of NCC from kapok fibres would add a new dimension to the adaptability of kapok fibres, allowing them to be employed in a variety of applications while also having a positive economic impact.

1.3.2 NCC isolation using acid hydrolysis

Obtaining NCC via acid hydrolysis, particularly with mineral acids such as sulphuric acid, involves the breaking of the β–1,4 glycosidic linkage of the glucose monomers in cellulose. During this process, hydronium ions can dissolve the amorphous regions in the microfibrils because the disordered amorphous regions are less densely packed than the crystalline regions, making them more susceptible to acid hydrolysis (Figure 1.3). The hydrolysis process in the amorphous regions can be achieved at faster hydrolysis kinetics due to a rapid drop in the number of repeated anhydrous glucopyranose units (AGUs) in cellulose. The level–off degree of polymerisation (LODP) is attained when the ordered crystalline areas reach the maximum hydrolysis yield and subsequent depolymerisation normally occurs at a slower rate (Habibi et al., 2010; Pandey et al., 2013).

Figure 1.4 shows the conventional acid hydrolytic procedure of lignocellulosic biomass for NCC production. The overall process typically commences with a constant mixing of cellulosic materials in a selected acid medium for a fixed period at an

elevated temperature, usually more than 40ºC. Following this, the reaction is terminated by neutralising the acidic mixture by adding a copious amount (~10-fold the amount of acid mixture) of cold water (~ 4ºC). Purification and isolation of NCC can be done by repeated centrifugation of the aqueous suspension or dialysis. After repeated centrifugation, the precipitated NCC can be neutralised with bases such as sodium hydroxide and ammonia before multiple centrifugations to remove free acids residues and salt produced. Following that, sonication may be used to improve the dispersion of the isolated nanoparticles (Bai et al., 2009; Dai et al., 2018; Ferreira et al., 2018). Finally, NCC might be dried to reduce their weight and shipping costs (Peng et al., 2012).

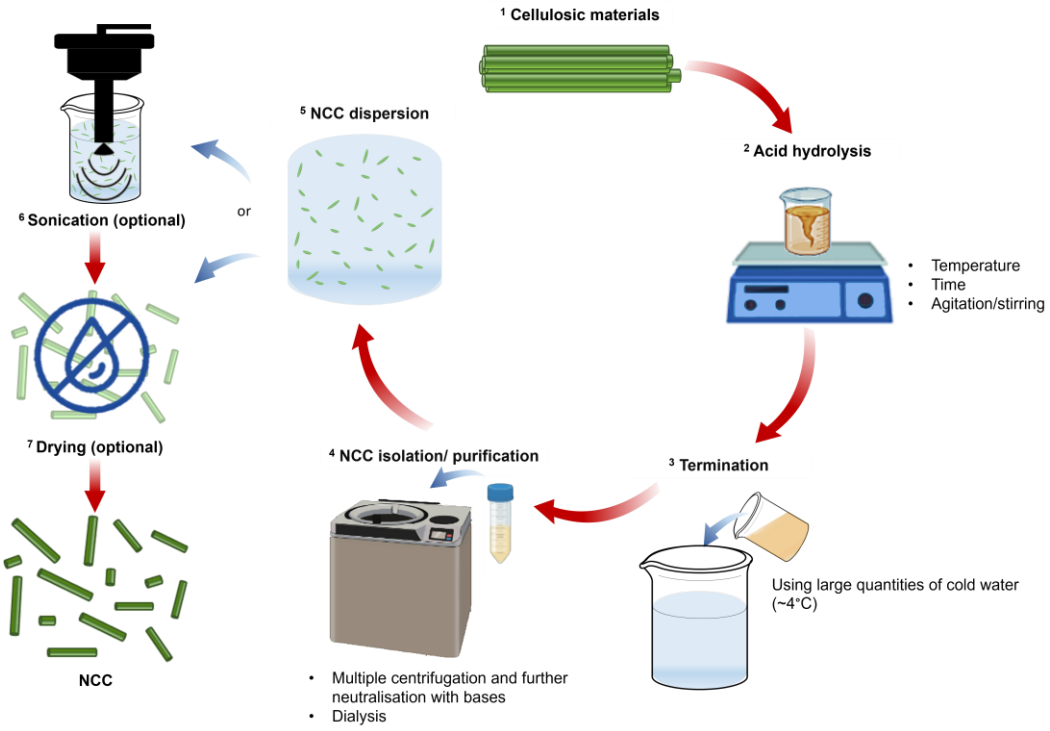

Figure 1.4 General procedure of acid hydrolysis for NCC extraction from cellulose feedstocks

Generally, the NCC produced via typical acid hydrolysis are extremely crystalline and exhibits a wide variety of dimensions (length: 100 – 500 nm; diameter:

5 – 50 nm). Furthermore, the dimensions and crystallinity index (CrI%) of NCC depend on the source of cellulose and the extraction conditions (Almashhadani et al., 2022; Le Gars et al., 2019).

It can conclude from the typical acid hydrolysis process that several key parameters, such as the type of biomass, acid concentration, reaction time, reaction temperature, acid-to-pulp ratio and sonication step, can be modified to generate NCC with the desired size and yield, as illustrated by the typical hydrolytic process (Bondeson et al., 2006; Dong et al., 2016; Dong et al., 1998). This is well indicated in Table 1.1 summarising the examples of cellulosic materials hydrolysed by sulphuric acid in the recent five years.

Table 1.1 Examples of acid hydrolysis using sulphuric acid for NCC extraction and related parameters

Cellulose source	Sulphuric acid concentration (%w/w, otherwise specified)	Acid-to-pulp ratio ($mL.g^{-1}$)	Reaction time (min)	Temperature (°C)	Sonication time (min)	Particle size (nm)		Yield (%)	Zeta potential (-mV)	Reference
						Length	Diameter			
Ampelodesmos mauritanicus fibres	64	20:1	60	45	–	108 ± 13	5.6 ± 1	55.7	28.5 ± 3.1	Zergane et al. (2020a)
Apple pomace	45	20:1	50	45	10	28 ± 2	8 ± 1	–	–	Melikoğlu et al. (2019)
Bamboo shoot (*Dendrocalamus asper*)	45 – 75	20:1	39	30 – 60	20	–	–	40 – 52	–	Wijaya et al. (2019)
Brazilian satintail (*Imperata Brasiliensis*)	50 – 64	(15 – 50):1	30 – 75	35 – 60	–	150 – 250	10 – 60	36 – 43	22 – 31	de Carvalho Benini et al. (2018)
Kapok fibres *(Ceiba pentandra)*	60	20:1	60	45	–	79 ± 12	4 ± 3	32	–	Mohamed et al. (2017)
Corncob	62	–	90	44	–	–	30 – 70	23.5	24.7 ± 0.8	Ditzel et al. (2017)
Corncob residue	64	–	60	45	–	147 – 249	3 – 8	34	33.8 ± 1.7	C. Liu et al. (2016)
Cotton fibres	64	11:1	45 – 55	50	–	125 – 140	–	32 – 41	- 0.3 µ/g [a]	Sun et al. (2016)
Eggplant plant (*Solanum melongena* L) residue	64	–	30	50	15	487 ± 154	6 ± 2	–	28.7	Bahloul et al. (2021)
Groundnut shell	65	20:1	75	45	–	67 – 172	5 – 18	12	–	Bano et al. (2017)
Industrial cotton waste	60	20:1	60 – 75	50	–	203 – 442	18 – 81	52 – 83	32 – 41	Maciel et al. (2019)
Industrial cotton waste	64	20:1	60 – 75	50	–	256 – 263	16 – 19	62 – 67	34 – 43	Maciel et al. (2019)
Mandacaru spines (*Cereus jamacaru DC.*)	60	–	60 – 120	45	–	260 – 400	25 – 30	–	–	Nepomuceno et al. (2017)
Napier grass (*Pennisetum purpureum*)	64	–	30 – 60	45	30	123 – 220	23 – 59	–	–	Sucinda et al. (2020)
Oil palm empty fruit bunch (OPEFB)	64	–	120	45	30	–	30 – 40	–	–	Azrina et al. (2017)
OPEFB	62	20:1	60	45	10	<50	–	–	–	Gan et al. (2017)
Pinecone (*Pinus Pinea*)	64	–	45	45	5	328 ± 82	2.9 ± 1	15	–	García-García et al. (2018)

Table 1.1 (Continued)

Cellulose source	Sulphuric acid concentration (%w/w, otherwise specified)	Acid-to-pulp ratio ($mL.g^{-1}$)	Reaction time (min)	Temperature (°C)	Sonication time (min)	Particle size (nm)		Yield (%)	Zeta potential (-mV)	Reference
Pineapple peel	64	20:1	45	50	–	189 ± 23	15 ± 5	21	–	Dai et al. (2018)
Sago seed shells	64	9:1	45	45	30	–	50 ± 3	–	37.8 ± 0.0	Naduparambath et al. (2018)
Solanum melongena L.	64	–	30	50	15	487 ± 154	6 ± 2	–	28.7	Bahloul et al. (2021)
Sugar palm	60	20:1	30 – 60	45	30	105 – 133	8 – 13	13 – 33	20 – 63	Ilyas et al. (2021)
Sugarcane bagasse fibres	60	20:1	75	45	120	200 – 300	20 – 40	–	–	Sukyai et al. (2018)
Sugarcane bagasse waste	65	25:1	45	45	15	413 ± 52	10 ± 3	–	32.3 ± 3.0	Ferreira et al. (2018)
Tea stalk	62	15:1	123	45	20	–	–	51	33.3	Guo et al. (2020)
Tomato plant residue	64	–	10 – 30	50	15	367 – 410	7 – 10	–	27 –37	Kassab et al. (2020)
Vine shoot	64	–	50	30	5	456 ± 123	14 ± 3	–	35.7	El Achaby et al. (2018)

Although considerable effort is being made to produce NCC using a variety of biomass using the most popular process, sulphuric acid hydrolysis, present NCC production is unlikely to meet the wide diversity of applications. Scaling up NCC production is complicated by a number of barriers faced during the acid hydrolysis process, including concerns about low yield, variation in the physiochemical properties of NCC and high production costs, which range between 3632 – 4420 USD/tonne of NCC (dry equivalent) (de Assis et al., 2017).

However, selecting biomass with a high cellulose content and optimising the acid hydrolysis parameters can be beneficial in producing NCC with the necessary physiochemical properties at relatively milder reaction conditions. As a result, several studies have been conducted to optimise NCC production and explore the interaction of parameters using experimental design and statistical analysis (de Carvalho Benini et al., 2018; Guo et al., 2020; Kargarzadeh et al., 2012; Wijaya et al., 2019).

1.3.3 Pharmaceutical applications of NCC

The lack of toxicity, the abundance of surface hydroxyl groups and the large surface area of NCC could make it an ideal carrier in medication delivery applications (Akhlaghi et al., 2013; Jackson et al., 2011). Therefore, many attempts have been reported to employ NCC as a suitable excipient for drug delivery (Gupta et al., 2020; Jackson et al., 2011) or carrier for API (Akhlaghi et al., 2013; Pourmoazzen et al., 2020). This is well indicated in Table 1.2 summarising the examples of NCC produced from different sources for drug delivery.

Table 1.2 NCC produced from different sources for drug delivery

Drug	Source of NCC	Method	Dosage form	Release manner	Reference
Docetaxel	Commercial softwood	i. Modifing the NCC with cetyl trimethylammonium bromide (CTAB) ii. Mixing CTAB- modified-NCC with docetaxel	Suspension	Sustained drug release with a total cumulative drug release of 59% after 2 days	Jackson et al. (2011)
Doxorubicin	Commercial softwood	Mixture of doxorubicin and NCC	Suspension	Rapid drug release over a 1 day	
Etoposide	Commercial softwood	i. Modifing the NCC with CTAB ii. Mixing CTAB- modified-NCC with etoposide	Suspension	Sustained drug release with a total cumulative drug release of 75% after 4 days	
Paclitaxel	Commercial softwood	i. Modifing the NCC with CTAB ii. Mixing CTAB- modified-NCC with paclitaxel	Suspension	Sustained drug release with a total cumulative drug release of 44% after 2 days	
Tetracycline	Commercial softwood	Mixture of tetracycline and NCC	Suspension	Rapid released over a 1 day	
Procaine	Commercial NCC	i. Surface modification of NCC with chitosan oligosaccharide ii. Chitosan modified NCC loaded with procaine hydrochloride	Suspension	Burst drug release of 80% of bound drug in the first hour followed by a slower release of drug over the following 1 h.	Akhlaghi et al. (2013)
Folic acid	Softwood	i. Amination of NCC ii. Binding of aminated NCC with fluorescein isothiocyanate (FTIC) to form NCC-FTIC iii. Mixing folic acid with NCC-FTIC in presence of 1-ethyl-3-(3-dimethylaminopropyl) carbodiimide and sucrose, N-hydroxysulfosuccinimide for 40h	Suspension	No data available	Dong et al. (2014)
Curcumin	Kenaf bast fibres	i. Modifing the NCC with CTAB ii. Mixing CTAB- modified-NCC with curcumin	Suspension	No data available	Zainuddin et al. (2017)
Diclofenac	*Citrus limetta albedo* peels	Modifing the NCC with CTAB Mixing with diclofenac	Suspension	Burst drug release of 30% during the first 20 min then followed by sustained release of 49.1% after 3h	Gupta et al. (2020)
Etodolac	*Citrus limetta albedo* peels	Modifing the NCC with CTAB Mixing with etodolac	Suspension	Burst drug release of 38% during the first 20 min then followed by sustained release of 54.6% after 3h	

Table 1.2 (Continued)

Drug	Source of NCC	Method	Dosage form	Release manner	Reference
IBU	*Citrus limetta albedo* peels	Modifing the NCC with CTAB Mixing with IBU	Suspension	Burst drug release of 29% during the first 20 min then followed by sustained release of 39.8% after 3h	Gupta et al. (2020)
Paracetamol	*Citrus limetta albedo* peels	Modifing the NCC with CTAB Mixing with paracetamol	Suspension	Burst drug release of 22% during the first 20 min then followed by sustained release of 38.4% after 3h	
Folic acid	Whatman paper #1	i. Surface-modification of NCC by nucleophilic reaction between cholesteryl chloroformate and hydroxyl group of NCC ii. Mixing the NCC-cholesterol with folic acid	Suspension	Burst drug release of 45% during the first 3 h then followed by sustained drug release of 55% after 2 days	Pourmoazzen et al. (2020)

Jackson et al. (2011) reported the application of NCC prepared from commercial softwood by acid hydrolysis as a drug delivery excipient for hydrophilic antibiotics doxorubicin and tetracycline. The mixtures of NCC-doxorubicin and NCC-tetracycline showed rapid release over 1 day. Moreover, they modified the surface of NCC with cetyl trimethylammonium bromide (CTAB) surfactant. After that, the hydrophobic anticancer drugs such as docetaxel, etoposide and paclitaxel were loaded with the CTAB-modified NCC solution and the drugs were released in a sustained manner over 2 days.

Another study conducted by Akhlaghi et al. (2013) oxidised a commercial NCC with 2,2,6,6-tetramethyl-1-(pyperidinyloxy) and then modified the surface of the oxidised NCC with chitosan to form an NCC-chitosan complex. The NCC-chitosan complex was used as a nanocarrier for a local anesthetic drug, procaine hydrochloride. The *in vitro* drug release from procaine-NCC-chitosan complex suspension at pH 8 showed a rapid release of 80% of the bound drug in the first hour, followed by a slower release of the drug over the following 1 h. The authors claimed that the chitosan-NCC complex could be a promising nanocarrier for pharmaceuticals in situations when rapid drug release is desired, such as buccal administration.

Recently, Gupta et al. (2020) used sulphuric acid hydrolysis to extract NCC from *Citrus limetta albedo* peels and then NCC was modified with CTAB surfactant to produce NCC-CTAB nanomaterials with a larger surface area and a high aspect ratio. The nanomaterials were then combined with four other anti-inflammatory drugs: etodolac, IBU, diclofenac and paracetamol. All nanomaterial suspensions studied show burst drug release (25 – 40%) in the first 20 min, followed by sustained drug release for 3 hours.

Pourmoazzen et al. (2020) produced NCC from Whatman paper # 1 by sulphuric acid hydrolysis and surface modification with cholesteryl chloroformate by a nucleophilic reaction to form a lipophilic matrix functioning as a host-guest release for folic acid. According to the findings, this NCC-cholesterol matrix loaded with folic acid exhibited sustained drug release for 2 days.

From work that has been done in the previous decade, NCC can be used as a drug nanocarrier either as a physical mixture or by modifying it with another agent such as a surfactant (CTAB) or cholesterol to alter the NCC hydrophilicity and then loading the drug to the modified NCC. Additionally, most studies examined the drug-NCC complex primarily for the oral route.

However, the application of NCC as a drug nanocarrier by direct binding of the drug to the NCC hydroxyl groups has not been investigated, especially for dermal delivery. Therefore, the current thesis will investigate the potential of NCC to be grafted directly with a drug moiety.

1.4 Design of experiment

The process of conducting an experiment involves various independent variables (factors) that influence the dependent variables (responses). The design of experiments (DoE) introduces an understanding of the relationships between experimental factors and their effects on the response, as well as the design of multidimensional experimental spaces (Anderson et al., 2016).

DoE aims to build a predictive model of all critical experimental factors and responses. Response surface methodology (RSM) is a commonly used mathematical and statistical technique for modelling and analysing processes in which the desired

response is affected by several variables with the goal of optimising the response using minimum number of experiments.

RSM includes different models to optimise the responses of a process, including central composite design (CCD) and Box-Behnken design, depending on the purpose and the number of factors to be tested. Box-Behnken designs have fewer design points than CCD (high, middle and low points), which may affect their prediction power (Bevilacqua et al., 2010; Ferreira et al., 2007). Therefore, the CCD model is a preferred method in the current thesis. The CCD contains five distinct levels for each factor:

i. High and low point (+1 and -1) of each factor.

ii. Central point (0) (the mean value of each factor) which enables an accurate estimation of the response curvature.

iii. Star points which are extremely high and low points (+ α and – α) of each factor (possible to estimate the quadratic term). The extreme values are determined according to the number of factors involved (Equation 1.1).

$$\alpha = [2^k]^{1/4} \qquad \text{Equation 1.1}$$

where *k* is the number of factors of the design.

For example, CCD with three factors can be represented as a cube; the vertices of the cube are the cube points and the centre of the cube is the design's central point. If the cube is assumed to be inscribed in a sphere, then, the star points define the sphere's ray. Figure 1.5 shows a graphical illustration of the CCD.

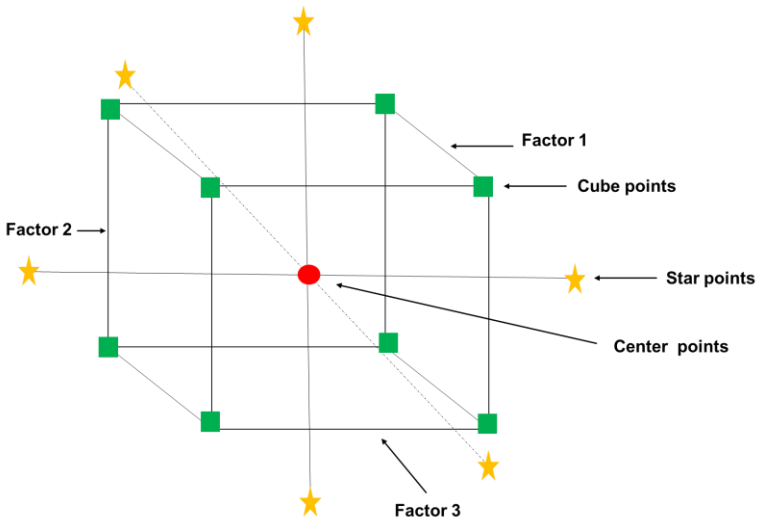

Figure 1.5 Schematic presentation of a three-factor CCD. Adapted from Bevilacqua et al. (2010)

Prior to beginning the discussion on the concepts and steps of RSM in the optimisation processing, it is necessary to define certain keywords (Yolmeh et al., 2017).

- Independent variables or factors are input variables that can be adjusted independently of one another.
- Dependent variables, or responses, are output variables affected by independent variables.
- The design space is the experimental range to be studied, which is defined by the upper and lower ranges of the independent variables.
- The experimental design is a set of experiments specified by a matrix including many level combinations of independent variables.

Figure 1.6 depicts the basic steps of the RSM, which are discussed briefly below:

i. Screening: To optimise an experiment that is affected by a broad range of factors, it is impractical and costly to evaluate the effect of each variable individually. To avoid this, the researcher may prefer to utilise a screening methodology to identify those variables with a significant impact on the response. Indeed, screening is the initial stage in the optimisation process. This step can be accomplished with either full or fractional factorial designs (Bezerra et al., 2008; Yolmeh et al., 2017).

ii. Selecting the process factors and their levels: After identifying the significant factors that affect the responses, the levels of the factors are determined. This stage is crucial to optimise the process and its success depends on its completion. Since the units and ranges of the factors are different, they must be determined before a regression analysis can be done (Bezerra et al., 2008).

iii. Regression model selection: Typically, the least-squares approach of multiple regression is used to analyse the relationship between independent and dependent variables (Ghorbannezhad et al., 2016).

iv. Verification of the fitted model: It is possible to calculate the estimated response using the model equation and regression coefficients. However, verification of the model adequacy must be checked to determine if it is appropriate or not. Several techniques are available, such as F-test of the model, lack of fit, coefficient of determination (R^2),

the difference between adjusted and predicted R^2 values and adequate precision (Bhattacharya, 2021).

v. Response modelling: Visualisation of the predicted responses can be seen by the response contour and surface graphs. These graphs are theoretical three-dimensional outputs of the RSM approach, which indicate the relationship between the dependent and independent variables (Bezerra et al., 2008).

vi. Selection and validation of the optimum condition (Bezerra et al., 2008).

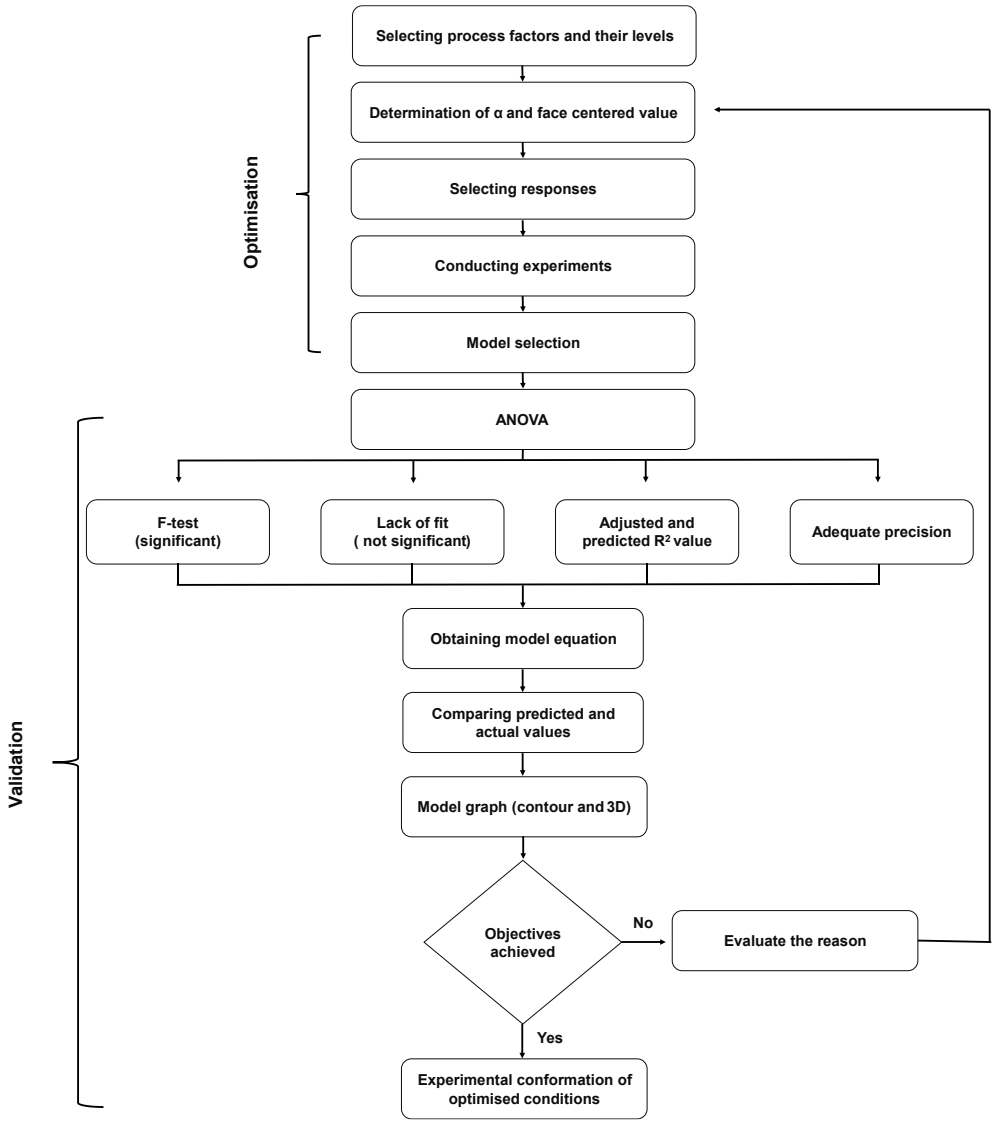

Figure 1.6 CCD flow diagram. Adapted from Bhattacharya (2021)

1.5 Electrospun fibres for dermal delivery

1.5.1 Introduction to electrospinning

Electrospinning is a straightforward and adaptable technology that utilises electrostatic forces to create extremely tiny polymer fibres ranging in size from submicron to nanoscale (Chen et al., 2022). The technique of electrospinning was first noticed by Rayleigh in 1897 and Zeleny explored it in-depth in the early 1900s (Zulkifli et al., 2022). After that, electrospinning has been emerged as an effective

technology for fabricating fibres with a nanosize diameter. Kenawy et al. (2002) pioneered the use of electrospun fibre mats as drug delivery vehicles using tetracycline hydrochloride (TCH) as a model drug, since then, electrospinning has grown in popularity for medical applications in the last two decades, particularly in nanofibre drug delivery systems (Chen et al., 2018).

The schematic diagram in Figure 1.7 illustrates the electrospinning of polymer fibres and the major components of typical electrospinning, including a syringe pump, a polymer solution, a metallic needle, a high voltage source and a collector. During the electrospinning process, a high voltage electric field is applied to the polymer liquid (a solution or suspension) resulting in the ejection of a continuous jet filament from the eluting needle that speeds toward the oppositely charged or grounded collector. In the absence of an electric field, the polymer droplet is retained at the tip of the needle by the polymer liquid surface tension. However, applying an electric field lead to countering the surface tension by electrostatic forces, causing the droplet to elongate and form into a cone known as a 'Taylor cone' (Rosell-Llompart et al., 2018). When the electrical field strength is strong enough to overcome the surface tension of the liquid, a fine fibre jet is launched from the tip of the Taylor cone. The solvent evaporates as the fibre jet travels through the atmosphere and solid polymer fibres are deposited as a solid, nonwoven, electrospun fibre mat on the collector (Hu et al., 2014).